RESEARCH ARTICLE
doi: 10.2306/scienceasia1513-1874.2025.097

ScienceAsia 51 (6): 2025: ID 2025097: **1–8**

Inhibin α association with multiple receptors and its role as a potential size regulator of Ningdu yellow rooster testis

Jishang Gong[a], Xuenong Zhu[a], Xinwei Xiong[a], Yuwen Tan[a], Yanping Wu[b], Jiguo Xu[a], Jinge Ma[a], Min Zhou[a,*]

[a] Jiangxi Provincial Key Laboratory of Poultry Genetic Improvement, Nanchang Normal University, Nanchang 330030 China

[b] Institute of Animal Husbandry and Veterinary Medicine, Jiangxi Academy of Agricultural Sciences, Nanchang 330030 China

[*]Corresponding author, e-mail: zhoumin@ncnu.edu.cn

Received 15 Apr 2024, Accepted 30 Nov 2025
Available online 22 Dec 2025

ABSTRACT: Inhibins play an essential role in gonadal development and are thought to strictly regulate gonad size. However, in poultry, the function and regulatory mechanisms of inhibin α (INHA) on testis size are unclear. In this study, testes of different sizes from 22-week-old Ningdu yellow roosters were used to evaluate the expression profiles of *INHA* and its related genes (*INHBA*, *ACVR2A*, *ACVR2B*, *FST*, *FSHR*, *LHR*, *AR*, and *AMH*). The INHA and the activin/inhibin receptor ACVR2A protein levels and cellular localization were also studied. The testis tissues were subjected to hematoxylin and eosin staining, immunofluorescence staining, and Western blotting. The expression of INHA and its related molecules was analyzed using quantitative PCR. Furthermore, protein interaction and gene ontology enrichment analyses were conducted. Compared to small testes, large testes showed bigger spermatogenic cells and seminiferous tubules; lower INHA and ACVR2A levels, especially in Leydig and spermatogenic cells; and lower expression of INHA and its related molecules. These results suggest that INHA may regulate testis size through receptor perception, particularly ACVR2A. This study provides reference information for breeding high-quality roosters.

KEYWORDS: testicular size, inhibin α, rooster, Ningdu yellow chicken

INTRODUCTION

For species with sexual reproduction, the ability to produce high-quality gametes is critical. During development, more is invested in testes quality than size in males in order to increase sperm competition [1]. Some researchers often ignore the animal's own genetic factors and try to improve the animal's spermatogenesis by adding drugs to increase reproductive hormones or testicular proteins [2]. However, the development of an individual and the cost of maintaining the testis tissue may affect testicular size. Males may choose to maximize trade-offs between testicular tissue investment and fertility, or to conserve or divert resources between future reproductive opportunities or other physiological and life-history characteristics [3]. No studies on testicular size differences in the same population have yet been reported. Investigating factors that may influence testes quality is critical for our understanding of the costs and benefits of sperm production and the mechanisms that regulate this process [4]. The testicular size of Japanese quail increased rapidly in the fifth week after hatching, and inhibin was found to be significantly elevated in plasma [5]. Under the influence of reduced light time, the testes of quail degenerated and became smaller, and the expression of inhibin subunits increased in the smaller testes [6]. The experimental results of Akhtar et al [7] showed that Yangzhou goose seminiferous epithelium underwent apoptosis after inhibin immunization and causing the seminiferous tubules to become smaller, thus affecting testicular size. The above literature shows that inhibin is correlated with the size of poultry testicles.

Inhibin is a glycoprotein hormone produced by the testes and ovaries to inhibit the synthesis and secretion of follicle-stimulating hormone (FSH) by the pituitary gland. As a result, inhibin is closely associated with sexual maturation in animals. Studies have shown that young children who received hematopoietic stem cell transplants had normal testosterone levels in adulthood, but testicular size was lower than normal, FSH levels were high, and inhibin B levels were low [8]. Inhibin B levels were also variable in patients with congenital hypogonadotropic hypogonadism and correlated with testicular size [9]. Ersoy et al [10] found that inhibin B concentration in newborn umbilical cord blood was positively correlated with testicular size. Jankowska et al [11] demonstrated a significant positive correlation between sperm count, serum levels of the inhibin β-subunit, and testicular size; in contrast, they reported a negative correlation between sperm count and FSH levels. These findings indicate that the inhibin β-subunit, along with FSH and testicular size, are critical markers of the competence of Sertoli cells and spermatogenesis in a man. This is in accordance with the findings of a few previous studies on the inhibin β-subunit and quality of spermatogenesis [12]. Zhang et al [13] used phylogenetic tree analysis to reveal that INHA and inhibin β-B (INHβB) evolved

independently. Through expression analysis of INHA, it was found that its expression in male testicles was higher than that of ovaries and pseudomale testes, while the expression of INHβB in ovaries was higher than that of male and pseudomale testes [13]. It was discovered that INHβB was accompanied by abnormal release in mice with smaller testes due to knockout of *Rnf216*/*Triad3* [14]. However, Zhao et al [15] increased *INHA* expression through *SPATA2* knockout, resulting in smaller testis and reduced weight in knockout mice compared with wild-type mice. In addition, the sperm count and reproductive cell proliferation of the knockout mice were decreased.

INHA was shown to play a critical role in regulating gonadal maturation both *in vivo* and *in vitro* [16–18]. Studies have shown that INHA stimulates the proliferation of Leydig cells cultured *in vitro*, promotes the secretion of androgens, and indirectly inhibits spermatogonia proliferation [19, 20]. We hypothesized that INHA regulation may influence the inhibin signaling pathway and the expression of related genes, affecting gonad phenotype and fecundity. In recent years, research on the role of INHA and activin has only focused on examining one hormone or subunit at a time; it greatly limits our understanding of the complex relationship between inhibin and their receptor.

Some researchers believe that *INHA* expression levels play a leading role in follicular development and participate in the regulation of reproductive traits in chickens [21]. Many studies have reported that INHA is a key regulator of gonadal function, but little is known about its effect on testes size. Few studies have examined *INHA* expression in testes of significantly different sizes to determine its potential role in sexual maturation and fertility [21].

To gain a better understanding of the role of INHA in male reproduction, we investigated testis tissues from 22-week-old Ningdu yellow roosters (a breed that can mature precociously at 16 weeks of age [22]) with significant differences in size within the same population. Ningdu yellow chicken is a Chinese landraces poultry breed with early sexual maturity and excellent meat quality and genetic performance [23]. Here, we examined protein localization and *INHA* and *ACVR2A* expression in tissues with large differences in chicken testicular volume, and the expression trends of related receptor genes were analyzed.

MATERIALS AND METHODS

Animals and tissue collection

Animal experimentation was carried out in accordance with the guidelines and ethics of the Nanchang Normal University Institutional Animal Care and Use Committee (NCNU-2022-006). Tissue samples for differences in testis size were collected by dissection from 500 reared 22 weeks old Ningdu yellow chickens (ad libitum intake of food). Ningdu yellow rooster (22 weeks old) with large testes ($n = 4$) and small testes ($n = 4$) were from a commercial layer farm in Nanchang. Parts of the tissues were fixed by 4% paraformaldehyde for morphological observation and subcellular location analysis using hematoxylin-eosin and immunofluorescence staining. Parts of tissues were stored immediately at −80 °C for mRNA and protein expression pattern analysis using quantitative real-time polymerase chain reaction (qRT-PCR) and Western blotting.

Hematoxylin-eosin (H.E.) staining

The testis tissues were embedded into paraffin (Solarbio, Beijing, China) and cut into 5 μm thickness sections using a microtome (Lecia, Weztlar, Germany). The sections were deparaffinized in xylene and rehydrated in an ethanol gradient. H.E. staining was carried out as described previously [24]. The images were captured using a Nikon Eclipse E100 microscope (Nikon, Tokyo, Japan).

Immunofluorescence staining

INHA and ACVR2A proteins were detected using an immunohistochemical standard avidinbiotin peroxidase method of the ABC staining system (Servicebio, Wuhan, China). Antigen retrieval was performed on dehydrated and transparent paraffin sections. Endogenous catalase deactivation was performed by immersion of the slides in 0.3% (v/v) hydrogen peroxide for 25 min at room temperature. After washing with PBS, 10% donkey serum was added and incubated at room temperature for 30 min. Rabbit polyclonal anti-INHA (1:3000, Servicebio) and anti-ACVR2A (1:500, Servicebio) were used to capture proteins and phosphate buffer solution (PBS, Servicebio) was used as a negative control, incubated at 4 °C overnight. After incubation with the primary antibody, samples were incubated with the appropriate HRP-conjugated secondary antibody (CY3 for INHA, FITC for ACVR2A, Servicebio) at a 1:250 dilution. Nuclei were counterstained with a 10 μg/ml DAPI. Images were captured using a Nikon Eclipse C1 microscope (Nikon). All immune-staining assays were performed at least in triplicate.

qRT-PCR

Total RNA was extracted from testes tissues using TransZol Up (TransGen Biotech, Beijing, China), 1 μg of total RNA was subjected to reverse transcription to single-stranded cDNA using EasyScript® One-Step gDNA Removal and cDNA Synthesis SuperMix (TransGen Biotech). The primers were designed using the Primer Premier 5.0 software, and were synthesized by Qinke Biotech Co., Ltd. (Wuhan, China). Primer sequences are shown in Table S1. qRT-PCR was performed using 2 μl of cDNA and TransStart® TipTaq (TransGen Biotech) in a 20 μl reaction volume on a Bio-Rad CFX96 real-time system (Bio-Rad, Hercules,

USA). *GAPDH* was used as an endogenous reference gene. A denaturation step run for one cycle at 94 °C for 30 s. The annealing step was run for 40 cycles at 94 °C for 5 s and 60 °C for 30 s. All PCR reactions were performed in triplicate. The results were calculated using the $2^{-\Delta\Delta CT}$ method [25].

Western blotting

Total protein was extracted from 100 mg of each tissue sample using RAPI (Servicebio). Protein concentration was determined using a BCA kit (Servicebio). A 100 μg sample was pipetted onto a sodium dodecyl sulfate polyacrylamide gel (SDS-PAGE) for Western blotting analysis. The blots were electrotransferred onto a polyvinylidene fluoride (PVDF) membrane (Millipore CAT, Billerica, MA, USA), and blocking by 1 M Tris-HCl buffer (pH 7.5) containing 5% (w/v) non-fat milk for 2 h at room temperature. The membranes were then incubated overnight at 4 °C with primary antibodies (1:1000): rabbit monoclonal anti-INHA antibody (Servicebio), rabbit monoclonal anti-ACVR2A antibody (Boster, Wuhan, China), and anti-β-ACTIN antibody (Servicebio). The subsequent procedures were carried out as described previously [24]. All immunoblot assays were performed at least in triplicate. Optical densities of the bands were quantified and scanned using Image-Pro Plus 6.0 (Media Cybernetics Co., Rockville, USA).

Gene ontology and Kyoto encyclopedia of genes and genome network analysis

Gene Ontology (GO) and Kyoto Encyclopedia of Genes and Genome (KEGG) network analyses were performed using g: Profiler software (https://biit.cs.ut.ee/gprofiler/gost) to identify overrepresented GO categories and pathway categories. The chord diagram was plotted by https://www.bioinformatics.com.cn, a free online platform for data analysis and visualization.

Statistical analysis

The data were presented as the mean ± SD, unless otherwise indicated. Statistical analysis was performed using SPSS version 24.0 (SPSS Inc., Chicago, IL, USA). The qPCR and Western blotting data were analyzed using the Student's test (between two groups) or one-way ANOVA analysis (within multiple groups). The graphs were drawn using Prism 5.0 (GraphPad Software Inc., San Diego, CA, USA). $p < 0.05$ was considered as statistically significantly different.

RESULTS

Testicular appearance and histological analysis

Overall, the collected testes were observed to vary in sizes (Fig. 1A), with significant differences in the weight of large and small testes of the left and right sides or both. No significant difference in total body weight was observed (Table 1). Comparative histological results showed that the seminiferous tubules of small testes were surrounded by tubular interstitial cells, and the lumen's seminiferous epithelium was composed of Sertoli cells and different spermatogenic cells (Fig. 1B). Most seminiferous epithelia have four layers of cells. The spermatogonia were round or oval and located close to the basement membrane, and the Sertoli cells were triangular or oval and slightly smaller than the spermatogonia (Fig. 1D). Primary and secondary spermatocytes were distributed in the second to third layers, and sperm cells and a small amount of sperm were in the uppermost layers (Fig. 1B,D).

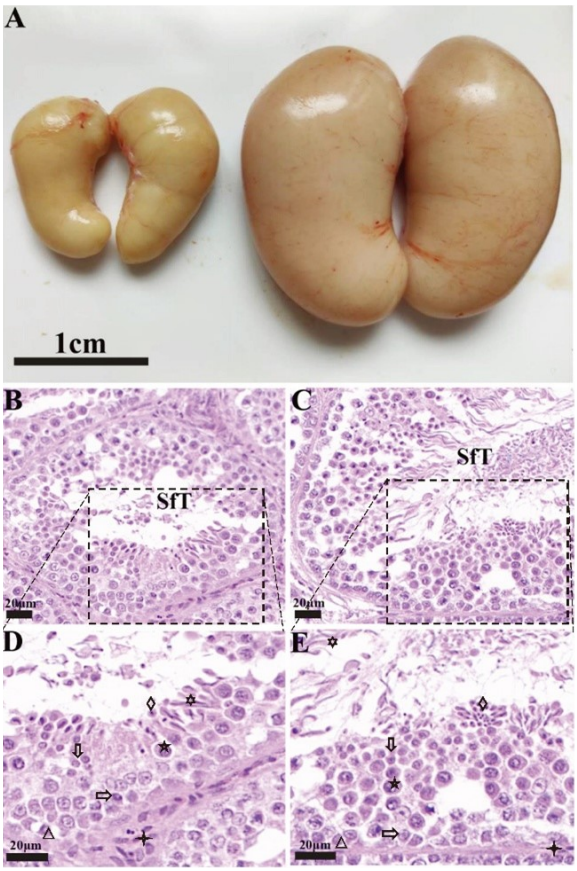

Fig. 1 The phenotype and H.E. staining of testes of different sizes. (A) Testicles of different sizes in 22 weeks; (B) to (E) Histological findings of: (B) the small testes under low power microscope; (C) the large testes under low power microscope; (D) the small testes under high power microscope; (E) the large testes under high power microscope. The horizontal arrow represents spermatogonia, the five-pointed star represents primary spermatocyte, vertical arrow represents secondary spermatocyte, diamond represents spermatid, hexagon represents spermatozoa, triangle represents Sertoli cell, the four-pointed star represents Leydig cells, SfT, seminiferous tubule.

Table 1 Comparison of testicular traits.

Age	Testicular phenotype ($n = 4$)	Body weight (g)	Left testis weight (g)	Right testis weight (g)	Testis weight (g)	Seminiferous tubule diameter (μm)
22 weeks	Small	1551.10 ± 342.67	3.90 ± 0.56[a]	3.23 ± 0.60[a]	7.13 ± 1.15[a]	218.74 ± 13.55[a]
	Large	1915.17 ± 332.17	31.00 ± 3.93[b]	29.93 ± 3.62[b]	60.93 ± 0.38[b]	356.61 ± 14.49[b]

Different letters in the same row indicate significant differences in relative expression ($p < 0.05$).

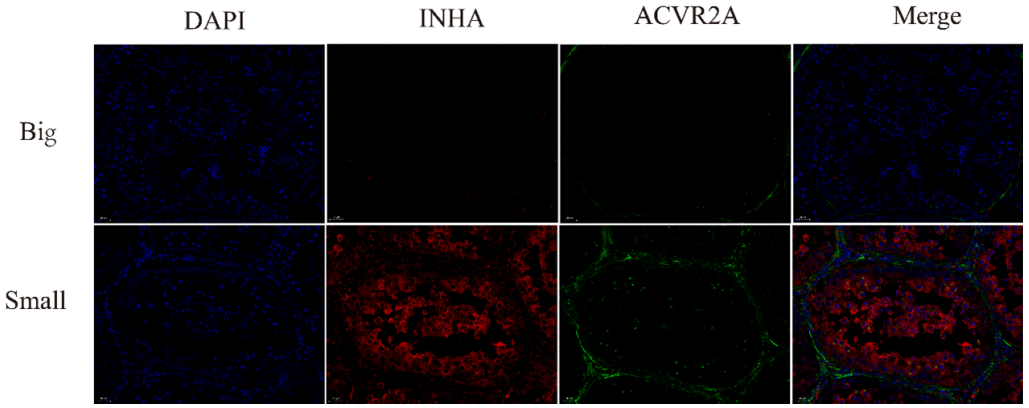

Fig. 2 Localization of INHA and ACVR2A in large and small testes using IF staining.

The seminiferous tubule diameters of large testes were significantly more extensive than those of small testes (Table 1), with a large number of spermatozoa in the lumen of each seminiferous tubule. Spermatogonia, primary spermatocytes, secondary spermatocytes, spermatids, and mature sperm cells were observed in the seminiferous tubules cross-section (Fig. 1C). Moreover, the spermatogonia were close to the basement membrane and arranged in a small, tight layer in most seminiferous tubules. The cells within this layer had a small, dense, and round or oval nucleus (Fig. 1E). The second layer of cells is the primary spermatocyte, showing a larger volume with a large nucleus. Primary spermatocytes were similar to secondary spermatocytes but with significantly smaller cell bodies and nuclei, smaller round spermatids, and a large number of mature spermatozoa in the seminiferous tubules (Fig. 1C,E).

Expression localization of INHA and ACVR2A in testis tissues of different sizes

INHA and ACVR2A cellular localization and distribution were analyzed using immunofluorescence staining to verify their relationship with the differences in testis size. Immunofluorescence of large and small testis tissues revealed that INHA was mainly expressed in small testes. Additionally, the INHA fluorescence was mainly distributed in the Sertoli cells, primary spermatocytes, and secondary spermatocytes of the seminiferous tubules epithelia (Fig. 2). The ACVR2A fluorescence was mainly observed in Leydig cells around the seminiferous tubules in small testis tissues. However, some primary spermatocytes and secondary spermatocytes in the lumen had a light fluorescence intensity next to their nuclei. Only weak ACVR2A fluorescence was observed in the Leydig cells of large testes.

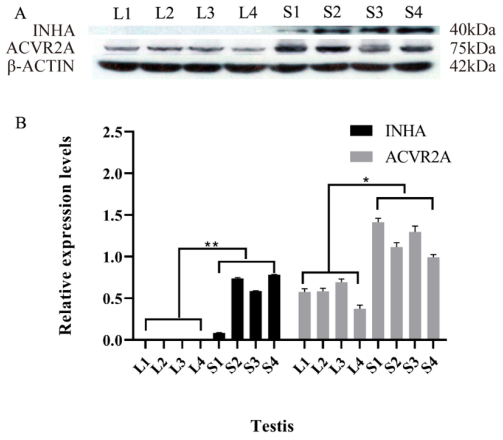

Fig. 3 Expression of INHA and ACVR2A in large (L1–4) and small (S1–4) testis tissues. (A) Immunoblotting results; (B) The IOD (Integrated Optical Density) values. * means $p < 0.05$, ** means $p < 0.01$.

Expression patterns of INHA and ACVR2A proteins in large and small testes

To further determine the differences in the expression levels of INHA and ACVR2A in large and small testes, immunoblotting experiments were performed. The results showed that INHA and ACVR2A expressions were significantly higher in small testes than in large

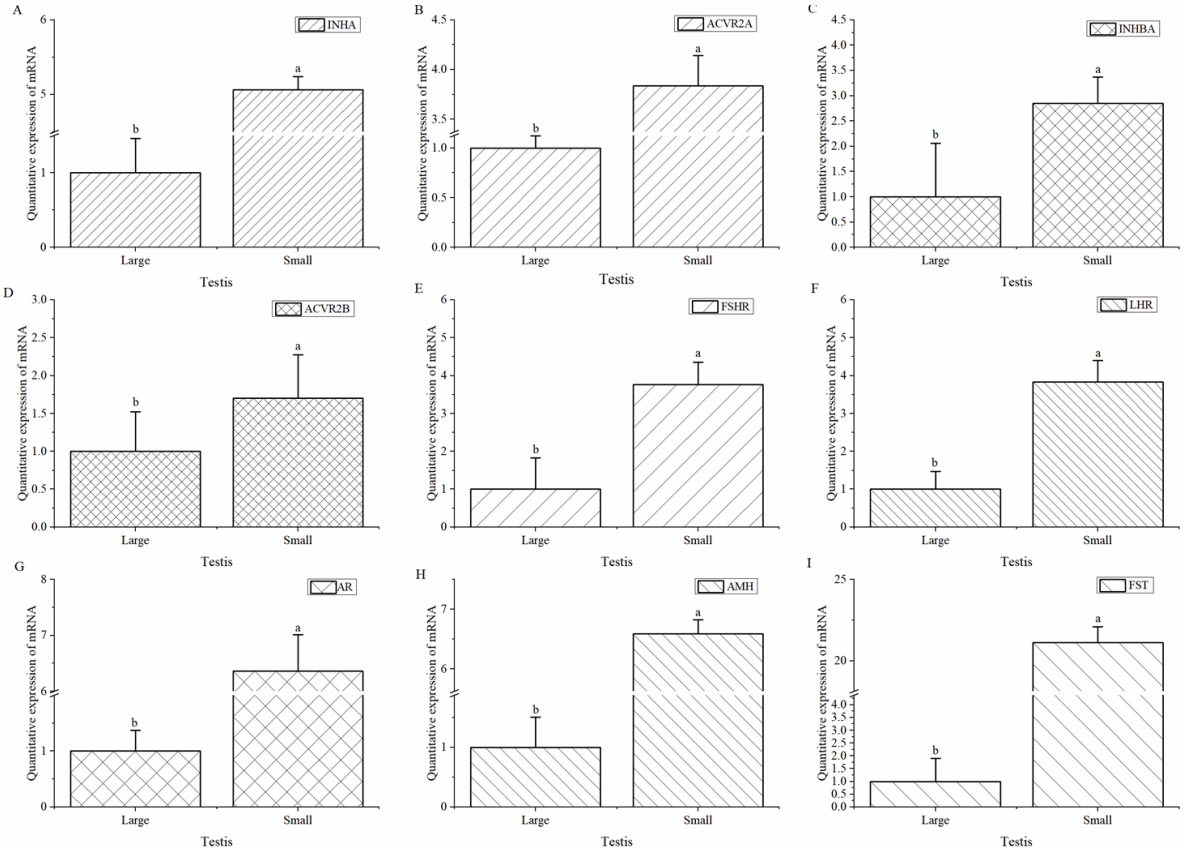

Fig. 4 Expression of INHA, ACVR2A INHBA, ACVR2B, FSHR, LHR, AR, AMH and FST in large and small testes tissues. Different letter means $p < 0.05$, same letter means $p > 0.05$.

testes, which showed only negligible levels of INHA (Fig. 3).

Expression levels of inhibin signaling pathway and reproduction-related genes in testes

We quantitatively analyzed the expression of eight genes related to INHA signaling using 22-week-old testis tissues to elucidate the relationship between the inhibin signaling pathway, testis size, and reproductive capacity (Fig. 4). The expression of *INHA* in large testes was significantly lower than that in small testes (Fig. 4A). The expression pattern of the activin receptor *ACVR2A* was similar to that of *INHA*, with the highest expression observed in small testes (Fig. 4B). *INHBA*, another subunit of inhibin, was significantly less expressed in large testes than in small testes (Fig. 4C). The *ACVR2B* expression pattern, one of the inhibin/activin receptors, was consistent with that of *INHBA*, i.e., with the highest expression level in small testes (Fig. 4D). Similarly, *FSHR*, *LHR*, *AR*, *AMH*, and *FST* (FSHR: Follicle-stimulating hormone receptor, LHR: Luteinizing hormone receptor, AR: Androgen receptor, AMH: Anti-Müllerian hormone, FST: Follistatin.) expressions in small testes were significantly higher than in large testes (Fig. 4E–I).

GO and KEGG network analysis

The GO enrichment analyses demonstrated that INHA and ACVR2A directly or indirectly participate in various biological processes associated with reproductive development, particularly gonadal development (Fig. 5). Moreover, INHA and ACVR2A may directly regulate cell population proliferation and cytokine-cytokine receptor interaction. INHA was mainly involved in hemoglobin-related biological processes, such as the hemoglobin biosynthetic process and hemoglobin metabolic process. ACVR2A participated widely in reproduction and development, such as in the development of the primary sexual characteristics, reproductive system, and male gonad. Altogether, we could speculate that INHA participated indirectly in the reproductive system development, reproductive structure development, reproductive process, and animal organ development by interacting with INHBA, ACVR2A, ACVR2B, FST, AMH, FSHR, and LHCGR, except AR.

DISCUSSION

Rooster fertility varies widely, and even within a flock, some males are extremely fertile, producing large

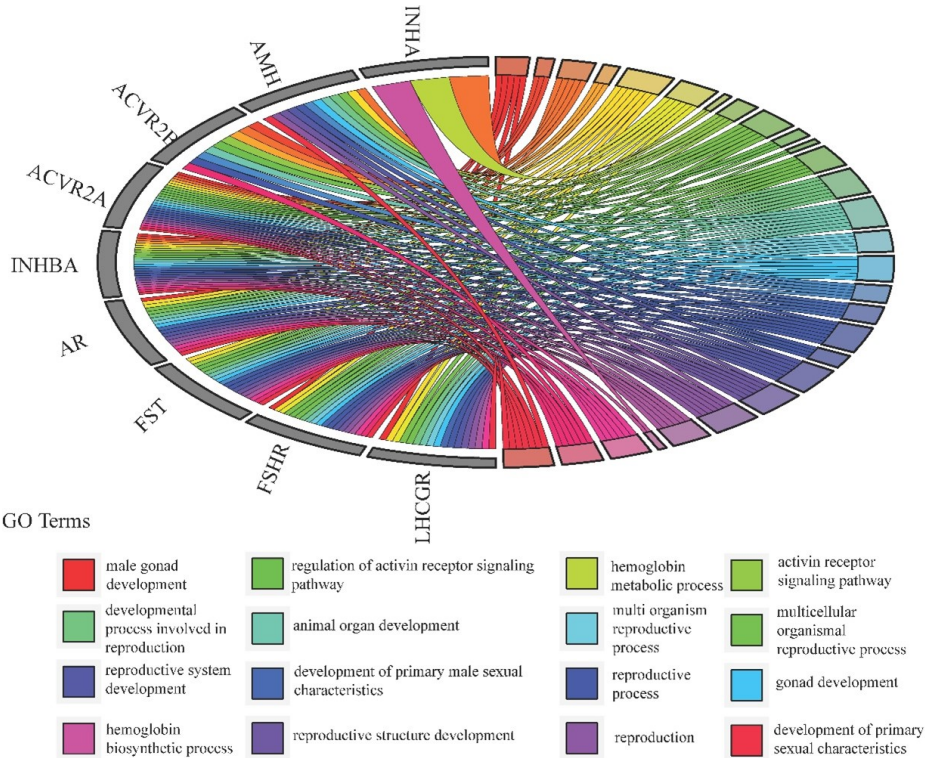

Fig. 5 GO enrichment functional analysis. Different colors represent different enrichment pathways.

quantities of high-quality sperm, whereas others are less fertile. Poultry testis size highly correlates with fecundity, and lower fecundity is often associated with small testes. Therefore, it is imperative to ensure the normal development of male testes. It can be accomplished by understanding the key regulators of male testis development. In this study, two groups of testes with significant differences in size were selected from 22-week-old roosters with no difference in body weight. Comparative histological results showed that the number of cells in the seminiferous tubules and the reproductive epithelium in small testes were significantly lower than those of large testes. This indicates that spermiogenesis is restricted due to developmental delays in small testes.

Immunofluorescence analysis using testes of different sizes showed that INHA and ACVR2A proteins were highly concentrated in small testes, and INHA was mostly observed in the seminiferous epithelium of seminiferous tubules. Western blotting and qRT-PCR showed that the expression of INHA in small testes was significantly higher than in large ones. Studies have shown that *INHA* downregulation has an antagonistic effect on granulosa cell apoptosis [26]. The five main stages of spermatogenesis are known to be spermatogonia, primary spermatocytes, secondary spermatocytes, spermatids, and spermatozoa [27]. The INHA expression was upregulated in small testis tissues, especially in spermatogenic cells, probably because small testes are still in an early developmental stage and the spermatogenic cells in seminiferous tubules proliferate slowly. ACVR2A was primarily immunoreactive in the Leydig cells, followed by a few spermatogenic nuclei in the small testes. ACVR2A was directly related to gonadal function in animals and can affect FSH levels in the body [28]. Although ACVR2A did not co-localize with INHA, both were upregulated in small testis tissues. This indicates that INHA and ACVR2A play regulatory roles in hypoplastic testes.

Furthermore, to understand the functional role of INHA, the expression profiles of the key molecules associated with INHA, such as INHBA, ACVR2B, FST, AR, FSHR, LHR, and AMH, were analyzed in testes of different sizes. The qRT-PCR results showed that the expression of the above seven INHA-related genes was significantly higher in small testes than in large testes. This suggests that *INHA* expression strongly correlates with animal reproduction and hormone regulation. INHBA is a subunit of the inhibin protein complex involved in developing the gonad [29]. In accordance with this, our results indicate that *INHBA* expression correlated with testis size traits and may regulate them together with INHA. ACVR2B, a receptor of the TGF-β superfamily, is considered the only candidate type II receptor that may mediate TGF-β signaling in gonadotropes [28]. According to our results, ACVR2B may be considered an inhibin receptor, as it showed a regulation trend consistent with the *INHA* expression

pattern. FST binding to activin and inhibin family members regulate their biological activity [30]. The expression pattern of *FST* in testes of different sizes was the same as that of *INHA*, suggesting that INHA may exert its biological function in combination with FST. AMH is also a member of the TGF-β superfamily, and studies have shown that it is highly expressed before puberty [31]. In our experiment, the expression of *AMH* in small testes was higher than in large ones. It is speculated that the small gonads enhance the expression of AMH in order to maintain reproductive capacity. FSHR and LHR are the main gonadotropin receptors through which FSH and LH function, respectively [32]. In this study, the *FSHR* and *LHR* expression levels were higher in small testes than in large ones. It is speculated that due to the high expression of FSHR and LHR, and possibly through the interaction with INHA, it has effect on the volume of the testis. Additionally, AR was also highly expressed in small testes, probably because the development of gonads requires large amounts of androgens that are perceived by their receptors, i.e., AR. Furthermore, GO enrichment analysis indicated that INHA indirectly regulates ACVR2A and participates in gonadal development.

CONCLUSION

This is the first study to show significant differential expression and cellular localization of INHA and ACVR2A in testes of different sizes. The expression of *INHA*, *ACVR2A*, *INHBA*, *ACVR2B*, *FST*, *FSHR*, *LHR*, *AR*, and *AMH* was significantly higher in small testes than in large testes, indicating that INHA may directly or indirectly affect the above hormone receptors, consequently affecting the size of poultry gonads. Based on the previously known functional role of INHA and ACVR2A in testis tissues and the expression profiles observed in the current study, we speculate that INHA may control spermatogenic cell differentiation required during gonadal development. Further studies are needed to determine INHA regulation in poultry spermatogenic cells and its potential functions in testes.

Appendix A. Supplementary data

Supplementary data associated with this article can be found at https://dx.doi.org/10.2306/scienceasia1513-1874.2025.097.

Acknowledgements: This work was supported by Jiangxi Provincial Department of Education Science and Technology Project (GJJ212618, GJJ212616), Joint research project of the Department of Agriculture and Rural Affairs of Jiangxi Province of China (2022JXCQZY03), and National Natural Science Foundation of China (32160784).

REFERENCES

1. Johnson TL, Symonds MRE, Elgar MA (2017) Anticipatory flexibility: larval population density in moths determines male investment in antennae, wings and testes. *Proc Biol Sci* **284**, 20172087.
2. Kang H, Gao M, Pei W, Wang S, Chen Z, Liu D (2024) Ginsenoside Rg1 improves spermatogenic dysfunction in cryptorchidism model rats by reducing blood-testis barrier damage. *ScienceAsia* **50**, ID 2024062.
3. Somjee U, Miller CW, Tatarnic NJ, Simmons LW (2018) Experimental manipulation reveals a trade-off between weapons and testes. *J Evol Biol* **31**, 57–65.
4. Vasudeva R, Deeming DC, Eady PE (2014) Developmental temperature affects the expression of ejaculatory traits and the outcome of sperm competition in *Callosobruchus maculatus*. *J Evol Biol* **27**, 1811–1818.
5. Sedqyar M, Weng Q, Watanabe G, Kandiel MM, Takahashi S, Suzuki A, Taneda S, Taya K (2008) Secretion of inhibin in male Japanese quail (*Coturnix japonica*) from one week of age to sexual maturity. *J Reprod Dev* **54**, 100–106.
6. Otake S, Park MK (2016) Expressional changes of AMH signaling system in the quail testis induced by photoperiod. *Reproduction* **152**, 575–589.
7. Akhtar MF, Ahmad E, Ali I, Shafiq M, Chen Z (2021) The effect of inhibin immunization in ieminiferous epithelium of yangzhou goose ganders: A histological study. *Animals* **11**, e-public.
8. Borgström B, Fridström M, Gustafsson B, Ljungman P, Rodriguez-Wallberg KA (2020) A prospective study on the long-term outcome of prepubertal and pubertal boys undergoing testicular biopsy for fertility preservation prior to hematologic stem cell transplantation. *Pediatr Blood Cancer* **67**, e28507.
9. Mosbah H, Bouvattier C, Maione L, Trabado S, De Filippo G, Cartes A, Donzeau A, Chanson P, et al (2020) GnRH stimulation testing and serum inhibin B in males: insufficient specificity for discriminating between congenital hypogonadotropic hypogonadism from constitutional delay of growth and puberty. *Hum Reprod* **35**, 2312–2322.
10. Ersoy B, Oval GY, Canda E, Onur E, Özyurt BC, Tansu N (2023) The relationship between ultrasonographically measured testicular volumes and cord blood inhibin B concentrations in healthy term male neonates. *Reprod Biol* **23**, 100786.
11. Jankowska K, Suszczewicz N, Rabijewski M, Dudek P, Zgliczyski W, Maksym RB (2022) Inhibin-B and FSH are good indicators of spermatogenesis but not the best indicators of fertility. *Life* **12**, 511.
12. Zhu ZG, Zhao ZG, Pang QY, Chen T, Zhang JM, Zhang TJ, Xu C, Zhang HB, et al (2019) Predictive significance of serum inhibin B on testicular haploid gamete retrieval outcomes in nonobstructive azoospermic men. *Asian J Androl* **21**, 137–142.
13. Zhang N, Dong Z, Xu W, Cui Z, Wang Q, Chen S (2020) Molecular characterization and expression pattern of inhibin α and βb in Chinese tongue sole (*Cynoglossus semilaevis*). *Gene Expr Patterns* **38**, 119148.
14. George AJ, Dong B, Lail H, Gomez M, Hoffiz YC, Ware CB, Fang N, Murphy AZ, et al (2022) The E3 ubiquitin ligase RNF216/TRIAD3 is a key coordinator of the hypothalamic-pituitary-gonadal axis. *iScience* **25**, 104386.
15. Zhao J, Zhao J, Xu G, Wang Z, Gao J, Cui S, Liu J (2017) Deletion of Spata2 by CRISPR/Cas9n causes increased

inhibin alpha expression and attenuated fertility in male mice. *Biol Reprod* **97**, 497–513.
16. Nagaraja AK, Middlebrook BS, Rajanahally S, Myers M, Li Q, Matzuk MM, Pangas SA (2010) Defective gonadotropin-dependent ovarian folliculogenesis and granulosa cell gene expression in inhibin-deficient mice. *Endocrinology* **151**, 4994–5006.
17. Suzumori N, Pangas SA, Rajkovic A (2007) Candidate genes for premature ovarian failure. *Curr Med Chem* **14**, 353–357.
18. Chang CL, Wang TH, Horng SG, Wu HM, Wang HS, Soong YK (2002) The concentration of inhibin B in follicular fluid: relation to oocyte maturation and embryo development. *Hum Reprod* **17**, 1724–1728.
19. Hsueh AJ, Dahl KD, Vaughan J, Tucker E, Rivier J, Bardin CW, Vale W (1987) Heterodimers and homodimers of inhibin subunits have different paracrine action in the modulation of luteinizing hormone-stimulated androgen biosynthesis. *Proc Natl Acad Sci USA* **84**, 5082–5086.
20. van Dissel-Emiliani FM, Grootenhuis AJ, de Jong FH, de Rooij DG (1989) Inhibin reduces spermatogonial numbers in testes of adult mice and Chinese hamsters. *Endocrinology* **125**, 1899–1903.
21. Cui Z, Liu L, Zhao X, Ran J, Wang Y, Yin H, Li D, Zhu Q (2019) Analysis of expression and single nucleotide polymorphisms of INHA gene associated with reproductive traits in chickens. *Biomed Res Int* **2019**, 8572837.
22. Mukhtar N, Khan SH (2012) Comb: An important reliable visual ornamental trait for selection in chickens. *World Poultry Sci J* **68**, 425–434.
23. Xiong X, Liu X, Zhu X, Tan Y, Wang Z, Xu J, Tu X, Rao Y, et al (2022) A mutation in PHKG1 causes high drip loss and low meat quality in Chinese Ningdu yellow chickens. *Poult Sci* **101**, 101556.
24. Gong J, Zhang Q, Wang Q, Ma Y, Du J, Zhang Y, Zhao X (2018) Identification and verification of potential piRNAs from domesticated yak testis. *Reproduction* **155**, 117–127.
25. Zhang Q, Wang Q, Gong J, Du J, Zhang Y, Zhao X (2018) Yak IGF2 promotes fibroblast proliferation via suppression of IGF1R and PI3KCG expression. *Genes* **9**, 169.
26. Chen F, Jiang X, Chen X, Liu G, Ding J (2007) Effects of downregulation of inhibin alpha gene expression on apoptosis and proliferation of goose granulosa cells. *J Genet Genomics* **34**, 1106–1113.
27. Sudtongkonga C, Kong-oha S, Wirachwonga P, Senaratb S, Kenthaoc A, Sukparangsid W, Kongtuenge P, Iidaf A, et al (2024) Male reproductive system and sperm ultrastructure of sesarmid crab *Episesarma singaporense* (Tweedie, 1936). *ScienceAsia* **50**, ID 2024054.
28. Schang G, Ongaro L, Schultz H, Wang Y, Zhou X, Brûlé E, Boehm U, Lee SJ, et al (2020) Murine FSH production depends on the activin type II receptors ACVR2A and ACVR2B. *Endocrinology* **161**, bqaa056.
29. Bao Y, Yao X, Li X, Ei-Samahy MA, Yang H, Liang Y, Liu Z, Wang F (2021) INHBA transfection regulates proliferation, apoptosis and hormone synthesis in sheep granulosa cells. *Theriogenology* **175**, 111–122.
30. Anderson RA, Evans LW, Irvine DS, McIntyre MA, Groome NP, Riley SC (1998) Follistatin and activin A production by the male reproductive tract. *Hum Reprod* **13**, 3319–3325.
31. Valeri C, Lovaisa MM, Racine C, Edelsztein NY, Riggio M, Giulianelli S, Venara M, Bedecarrás P, et al (2020) Molecular mechanisms underlying AMH elevation in hyperoestrogenic states in males. *Sci Rep* **10**, 15062.
32. Burow S, Mizrahi N, Maugars G, von Krogh K, Nourizadeh-Lillabadi R, Hollander-Cohen L, Shpilman M, Atre I, et al (2020) Characterization of gonadotropin receptors Fshr and Lhr in Japanese medaka, *Oryzias latipes*. *Gen Comp Endocrinol* **285**, 113276.

Appendix A. Supplementary data

Table S1 Primers using for qPCR.

Gene	Gene accession no.	Primer name	Primers sequence (5′ → 3′)
INHA	NM_001031257	INHA-F	TGAGGAGCAGGAGGACACATC
		INHA-R	GGGCTGGAAGAGGTAAGTGAAG
ACVR2A	NM_205367	ACVR2A-F	AAGCGAGGCACCAGCATTGATGT
		ACVR2A-R	GCCAAGCCTCGAGCCATAGTCTG
INHBA	NM_205396	INHBA-F	TGGGAAAGGTGGGAGATGATGG
		INHBA-R	CCTGCTCCGGTTGGCCTTGG
ACVR2B	NM_204317	ACVR2B-F	CGCCCTCCCTGCTTAACATCCTG
		ACVR2B-R	GGCCGGGGTCCTCATTGATGTC
AMH	NM_205030	AMH-F	CGCCGTGAGCAGCAGCAGCAAG
		AMH-R	CCCGGCCAGCAGGAGCAGCAC
FST	NM_205200	FST-F	CCCAGGCAGCTCCACGTGTGT
		FST-R	TTCGCTTTGATGCATTTTCCCTC
AR	NM_001040090.2	AR-F	AGAAGCTGGGCAGTCTGAAG
		AR-R	CAAAGCCATTGACGTGTGTC
FSHR	NM_205079	FSHR-F	CATGGGATACAACGTGCTGAGAG
		FSHR-R	CCGGCTTTTGGTCTGGATATCTAC
LHCGR	NM_204936	LHCGR-F	GGATACACAACGATGCCCTGAGAG
		LHCGR-R	AATTTATCCAGAGGCGGCAGTC
GAPDH	NM_204305	GAPDH-F	CGCCATCACTATCTTCCAGGAGC
		GAPDH-R	CGCTTAGCACCACCCTTCAGATG